photonics

MDPI

Communication

A High-Peak-Power Mechanically Q-Switched Tb:$LiYF_4$ Laser in the Green Spectral Region

Linpeng Yu [1], Haotian Yang [2], Hiyori Uehara [1,2] and Ryo Yasuhara [1,2,*]

[1] National Institute for Fusion Science, 322-6 Oroshi-cho, Toki 509-5292, Japan; yu.linpeng@nifs.ac.jp (L.Y.); uehara.hiyori@nifs.ac.jp (H.U.)
[2] The Graduate University for Advanced Studies, SOKENDAI, 322-6 Oroshi-cho, Toki 509-5292, Japan; yang.haotian@nifs.ac.jp
* Correspondence: yasuhara.ryo@nifs.ac.jp

Abstract: We report on a mechanically Q-switched Tb:$LiYF_4$ laser at 544 nm based on an optical chopper. With appropriate chopper settings, 521 μJ, 86 ns green pulses are generated at 1 kHz, corresponding to a peak power of 6.1 kW. To the best of our knowledge, this is the highest peak power generated using Tb:$LiYF_4$ lasers to date. Numerical simulations are carried out and agree well with the experimental results, which show that the pulse energy can be further scaled to the millijoule level and the peak power to over 10 kW.

Keywords: terbium; Q-switched; green laser; high peak power

1. Introduction

Recently, many efforts have been devoted to the development of green lasers owing to their wide scientific and industrial applications, such as material processing, medical treatment, optical communication and laser imaging [1–6]. Various methods have been proposed for achieving green light emissions, including nonlinear frequency conversion and direct laser emissions from rare-earth-doped (Pr^{3+}, Tb^{3+}, Dy^{3+}, Ho^{3+} and Er^{3+}) gain media [7–9]. Compared with nonlinear-frequency-conversion-based light sources, in which complex laser designs are required, directly emitting green solid-state lasers are potentially more attractive due to their compactness, simplicity and higher efficiency. To date, based on rapidly developed frequency-doubled optically pumped semiconductor lasers (2ω-OPSLs), the highest continuous-wave (CW) average power from Pr^{3+}-doped lasers can reach 4.3 W [10], while this is 1.25 W for Tb^{3+}-doped lasers [11].

For a number of high-precision applications, to avoid collateral damage to the peripheral elements, green pulsed lasers with a short pulse duration and a high peak power are desired prior to CW operation. Q-switching has been demonstrated to be a common and reliable technique for generating short and intense pulses. Among all of the rare earth ions with green transition, trivalent terbium (Tb^{3+}) is a good candidate for Q-switched laser applications owing to its long upper-state lifetime and low non-radiative loss, which allow for large energy storage [12]. Meanwhile, the upper $^5D_4$ state of Tb^{3+} does not suffer a concentration-quenching effect, indicating that the substrate crystals can be highly doped [12]. The high doping concentration can further enhance the energy storage capability of Tb^{3+}-doped lasers. To date, several works concerning Q-switched Tb^{3+}-doped lasers have been reported. Chen et al. realized the first passively Q-switched Tb^{3+}-doped lasers in the green spectral region by using a single-layer graphene saturable absorber (SA), which produced 2.9 μs, 19.2 μJ Q-switched pulses at 38.7 kHz, corresponding to a peak power

check for updates

Received: 20 December 2024
Revised: 8 January 2025
Accepted: 9 January 2025
Published: 10 January 2025

Citation: Yu, L.; Yang, H.; Uehara, H.; Yasuhara, R. A High-Peak-Power Mechanically Q-Switched Tb:$LiYF_4$ Laser in the Green Spectral Region. *Photonics* **2025**, *12*, 58. https://doi.org/10.3390/photonics12010058

of 6.6 W [11]. Afterwards, with a Co^{2+}:$MgAl_2O_4$ crystal as the SA, the output peak power was further scaled to hundreds of watts with a sub-μs pulse duration [13,14].

Compared with passive Q-switching, active Q-switching has the clear advantages of a controllable pulse repetition rate, a larger output pulse energy and higher peak power. Employing an acousto-optic modulator (AOM) [15] and an electro-optic modulator (EOM) [16], actively Q-switched Tb^{3+}-doped lasers have been demonstrated. Specifically, the AOM-based Q-switched laser could deliver 0.15 mJ pulses at 3 kHz with a peak power of 0.58 kW, while the EOM-based Q-switched laser could generate 0.2 mJ pulses at 200 Hz with a higher peak power of 0.8 kW. However, in addition to their high costs and bulky systems, the insertion of the AOM and EOM will cause an additional cavity loss, which will degrade the laser performance. Considering these deficiencies, more efforts are required to address the need for an economic and compact Q-switched Tb^{3+}-doped laser with a high output peak power.

Mechanical Q-switching, especially optical chopper Q-switching, represents a simple approach to realizing high-peak-power pulsed operation [17–20]. Mechanical Q-switches comprise inexpensive and readily available components which are unsusceptible to laser-induced damage and maintenance-free. More importantly, when working in a high-Q state, mechanical Q-switches exhibit no cavity insertion loss. This paper will show our recent efforts towards developing a mechanically Q-switched Tb:$LiYF_4$ laser. The laser adopts an optical chopper as the Q-switch and generates green pulses with a pulse energy of 521 μJ and a pulse duration of 86 ns at 1 kHz, corresponding to a peak power of 6.1 kW. To the best of our knowledge, this is the highest peak power generated using Tb:$LiYF_4$ lasers to date. Numerical simulations agree well with the experimental results and predict the generation of millijoule pulses with a peak power in excess of 10 kW.

2. The Experimental Setup

A schematic of the experimental setup is depicted in Figure 1. A hemispherical cavity is constructed, which is composed of a planar input mirror (IM, HT@488 nm, HR@544 nm) and a concave output coupler (OC, HR@488 nm). The OC has a transmittance of 3.6% at 544 nm and a radius of curvature of 100 mm. The pump source is a commercial 2ω-OPSL (Coherent Genesis CXSTM) that can output a maximum power of 3 W at 488 nm. A half-wave plate is inserted to adjust the polarization of the pump light for optimization of the laser's efficiency. The pump's light is focused onto a commercial c-cut 15% Tb:$LiYF_4$ (Tb:YLF, EKSMA Optics, Vilnius, Lithuania) crystal using a plano-convex lens (f = 500 mm), resulting in a beam radius of 77 μm with a Rayleigh range of 34.5 mm. The Tb:$LiYF_4$ crystal has a length of 30 mm and an aperture of 5 mm, with both surfaces anti-reflection-coated, and is placed as close as possible to the IM. The single-pass absorption efficiency of the pump light in the gain crystal is measured to be 56%. Considering the second-pass absorption benefiting from the high reflectance at 488 nm of the OC, a total absorption efficiency of 81% can be obtained in the CW operation state. Residual light from the pump is blocked using a long-pass filter (FEL0500, Thorlabs, Newton, NJ, USA). An optical chopper is placed between the crystal and the OC. In the experiment, we select two types of choppers (Chopper 1: Thorlabs MC1F100, a 50% duty cycle, frequency adjustable from 200 Hz to 10 kHz; Chopper 2: Thorlabs MC1F10A, adjustable 10-slot blade with a 0–50% duty cycle, frequency adjustable from 20 Hz to 1 kHz) and study the influences of the chopper frequency and duty cycle on the laser performance. To achieve good mode-matching between the pump and the laser modes, the total cavity length is adjusted to approximately 100 mm. The corresponding TEM_{00}-mode beam radius is calculated to be 71 μm, indicating good spatial overlap between the pump mode and the laser mode.

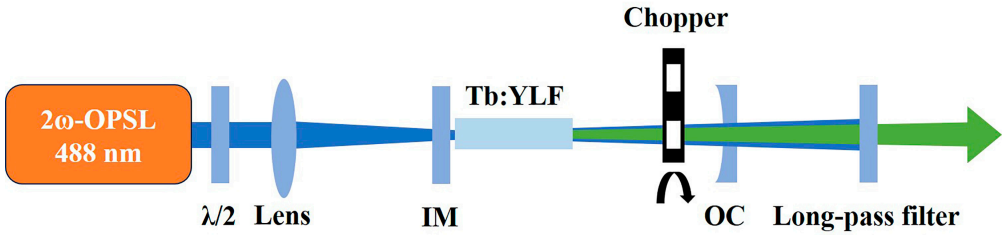

Figure 1. Schematic of the mechanically Q-switched Tb:$LiYF_4$ laser. $\lambda/2$: half-wave plate; IM: input mirror; OC: output coupler.

The temporal characteristics of the Q-switched pulses are monitored using a silicon-based photodetector (Thorlabs DET10A/M, Newton, NJ, USA, rise time = ~1 ns) connected to a digital oscilloscope (Keysight, MSOX3024T, Santa Rosa, CA, USA, bandwidth: 200 MHz). The spectrum is measured using an optical spectrum analyzer (Ocean Optics, USB2000, Orlando, FL, USA).

3. Results and Discussion

The dependence of the average output power on the incident pump power in different Q-switched states is illustrated in Figure 2a. It is seen that with a chopper frequency of 10 kHz and a duty cycle of 50%, the output power increases linearly with the incident pump power without the appearance of saturation. A maximum output power of 874 mW is obtained, while the corresponding slope efficiency reaches 35%. To the best of our knowledge, this is the highest average power generated using Q-switched Tb:$LiYF_4$ lasers to date, demonstrating the good advantages of optical chopper Q-switching. When the chopper frequency is reduced to 1 kHz, the maximum output power and slope efficiency decrease to 685 mW and 27%, respectively. Meanwhile, multiple pulses are observed at the trailing edge of the main pulse, as shown in the middle panel of Figure 2b. Generally, this multi-pulse phenomenon is caused by the long switching time of the Q-switch [21]. To mitigate the multi-pulse problem, we adjust the duty cycle to 10% while maintaining the chopper frequency at 1 kHz. As a result, the maximum output power and slope efficiency drop to 521 mW and 21%, respectively, whereas the trailing pulses disappear, as shown in the bottom panel of Figure 2b. However, due to the inherent mechanical instability of optical choppers, significant pulse-to-pulse amplitude fluctuations are observed. With a chopper frequency of 1 kHz and a duty cycle of 10%, the normalized root mean square (RMS) deviation in the pulse amplitude is calculated to be 24.4%, while it is 28.3% and 21.6% for the cases of 1 kHz (50%) and 10 kHz (50%), respectively. For comparison, we also present the results in the CW state in Figure 2a, which are characterized by a maximum output power of 1.02 W and a slope efficiency of 41%. Taking into account the absorption efficiency of 81%, the slope efficiency with respect to the absorbed pump power can reach 51%.

Figure 3a depicts the measured pulse duration as a function of the incident pump power. As the pump power increases, the pulse duration gradually decreases, while a lower chopper frequency or a smaller duty cycle favors a shorter pulse duration. This is due to the fact that a higher pump power, a lower chopper frequency or a smaller duty cycle can help store more energy in the gain medium and thus provide a higher roundtrip gain, which, in turn, generates a laser pulse for fewer round trips [22]. The shortest pulse duration of 86 ns is obtained with a chopper frequency of 1 kHz and a duty cycle of 10%. Note that to prevent optical damage to the coatings due to the high intra-cavity pulse energy, the chopper frequency and the duty cycle in the experiment are kept above 1 kHz and 10%, respectively. Figure 3b,c present the corresponding single-pulse waveform and spectrum, respectively. The center wavelength is located at 544 nm. No noticeable change

in the laser wavelength is observed in the experiment regardless of the chopper frequency or duty cycle.

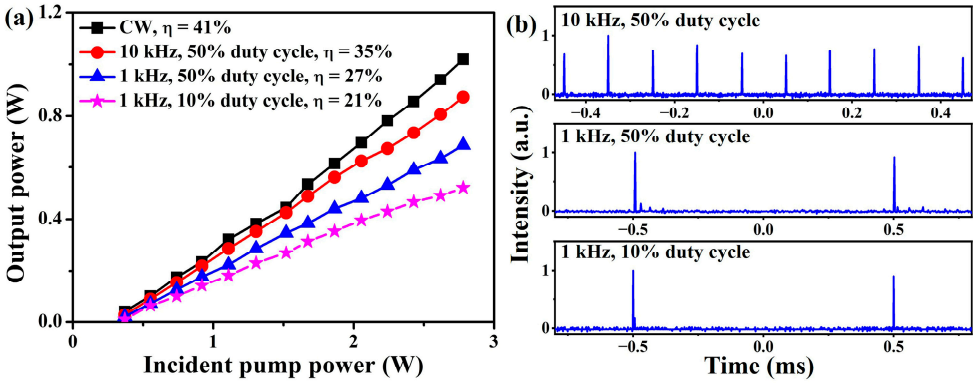

Figure 2. (**a**) Average output power of the Tb:$LiYF_4$ laser in the CW state and different Q-switched states. (**b**) Typical pulse trains under different chopper frequencies and duty cycles.

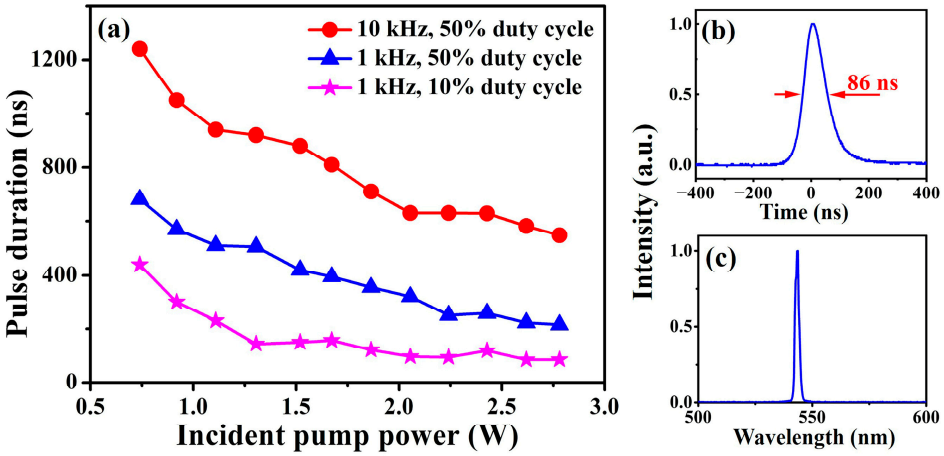

Figure 3. (**a**) Measured pulse duration versus incident pump power under different chopper frequencies and duty cycles. (**b**) Pulse waveform and (**c**) corresponding spectrum at shortest output pulse duration.

To explore the peak power scalability, a further discussion is carried out based on the setting of 1 kHz and a 10% duty cycle. Figure 4a depicts the evolution of the experimentally obtained pulse energy with the incident pump power. Under the maximum available pump power, the largest pulse energy reaches 521 μJ. The corresponding calculated peak power is shown in Figure 4b, which increases with an increasing pump power, generating a record peak power of 6.1 kW. Compared with the sub-kW peak power from AOM- and EOM-based Q-switched Tb:$LiYF_4$ lasers [15,16], the output peak power from this laser is greatly enhanced. For a better understanding of the pulse dynamics in mechanically Q-switched Tb:$LiYF_4$ lasers, numerical simulations are also carried out. The intracavity photon density ϕ and population inversion density n can be described using the coupled differential equations [23]

$$\begin{aligned} \frac{d\phi}{dt} &= \frac{2\sigma n l \phi}{t_r} - \frac{\phi}{t_c} \\ \frac{dn}{dt} &= -\gamma \sigma c \phi n \end{aligned}, \quad (1)$$

where $\sigma = 2 \times 10^{-21}$ cm^2 is the stimulated emission's cross-section [12], c is the speed of light in a vacuum, l is the length of the gain crystal, and $t_r = 2l'/c$ is the roundtrip transit time in the laser cavity of length l'. The inversion reduction factor γ is set to 1 due to the

rapid multi-phonon relaxation of the lower $^7F_5$ state of Tb^{3+} [24]. The photon decay time t_c can be expressed as

$$t_c = \frac{t_r}{\left[\ln\left(\frac{1}{R}\right) + L\right]}, \tag{2}$$

where R is the OC's reflectivity, and L = 5% is the roundtrip dissipative optical loss. To determine the initial and final population inversion densities n_i and n_f relative to the pulse build-up process, an additional equation is required to describe the accumulation behavior of n during the time interval between sequent pulses, which can be written as [25]

$$\frac{dn}{dt} = KP_{\text{in}} - \frac{n}{\tau}, \tag{3}$$

where P_{in} is the incident pump power, and τ = 4.9 ms is the fluorescence lifetime [16]. $K = \eta n_t / \tau P_{th}$ is a pumping parameter, in which η is the absorption efficiency and Pth is the threshold pump power. n_t is the threshold inversion density and can be obtained using

$$n_t = \frac{1}{2\sigma l}\left[\ln\left(\frac{1}{R}\right) + L\right]. \tag{4}$$

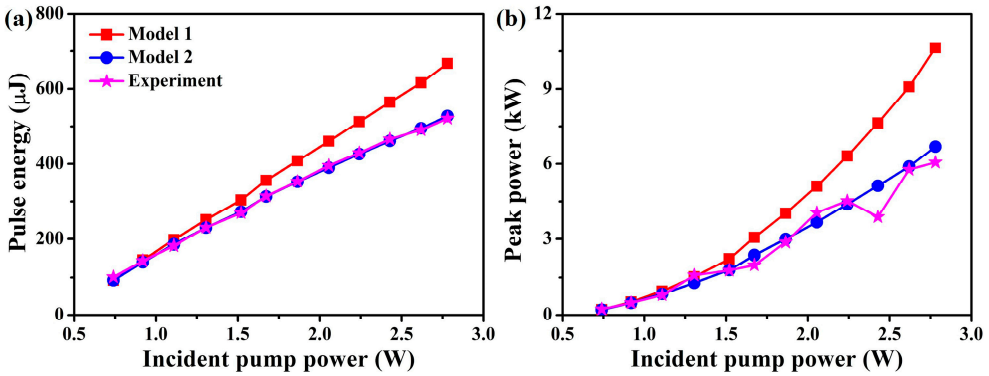

Figure 4. (**a**) Pulse energy and (**b**) peak power versus incident pump power with a chopper frequency of 1 kHz and a duty cycle of 10%. The numerical results of Model 1 (red square) and Model 2 (blue circle) are compared with the experimental results (magenta pentagram).

After numerically solving the above equations, the single pulse energy and peak power can be calculated by using the formulas [23]

$$E = \frac{hvA}{2\sigma\gamma}\ln\left(\frac{1}{R}\right)\ln\left(\frac{n_i}{n_f}\right), \tag{5}$$

$$P = \frac{Alhv}{\gamma t_r}\ln\left(\frac{1}{R}\right)\left[n_i - n_t - n_t\ln\left(\frac{n_i}{n_t}\right)\right] \tag{6}$$

where A is the beam's cross-section area, and hv is the laser photon energy. Generally, Pth is treated as a constant. Figure 4 shows the corresponding calculated results according to Equations (5) and (6), which are labeled Model 1. In order to bring the simulation into better agreement with the experiment, here, we introduce a dimensionless coefficient α and assume that $Pth = \alpha \times P_{in} + P_0$. This assumption can be explained by the possibility that as the incident pump power P_{in} increases, the thermal lens effect will become severe and cause a mode mismatch between the pump and the laser beam, which will result in an increase in the threshold pump power Pth [26,27]. The corresponding calculated results, labeled Model 2, are also shown in Figure 4 for comparison. It is seen that Model 2 is more

consistent with the experimental results than Model 1, exhibiting a good tool for studying the Q-switched pulse dynamics.

The evolution of the population inversion density n during the pulse build-up process under the maximum pump power is illustrated in Figure 5a. It is seen that n decreases slowly first and then rapidly. When n drops to the threshold inversion density n_t, the instantaneous power coupled from the cavity reaches its peak value. In other words, the maximum intracavity photon density ϕ is obtained when the gain is equal to the loss. Beyond the threshold point, the instantaneous power dies out quickly, generating a Q-switched pulse with a pulse duration of 79 ns and a peak power of 6.7 kW. The slight inconsistency with the experiment may be caused by pulse-to-pulse instability in the experiment or inaccuracies in the simulation parameters. Afterwards, the population inversion density n starts to recover under the pump radiation and enters the next cycle.

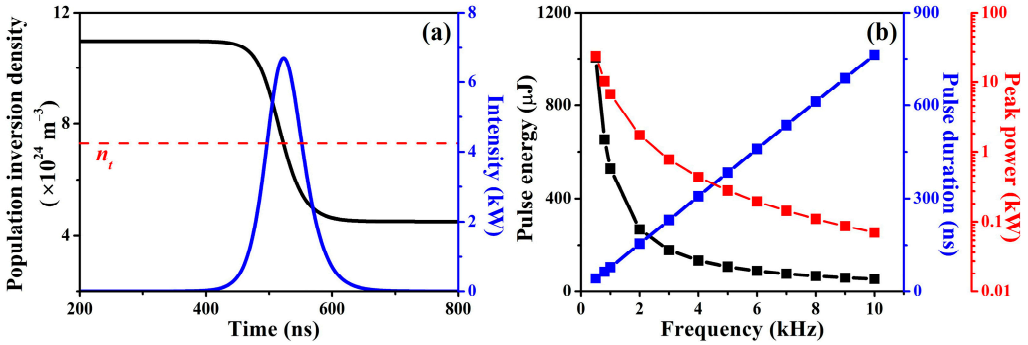

Figure 5. (**a**) Evolution of population inversion density n and instantaneous power coupled from the cavity during one roundtrip. (**b**) Numerically obtained pulse energy, pulse duration and peak power as a function of the chopper frequency.

The output pulse characteristics at different chopper frequencies under a fixed pump power of 3 W are numerically investigated based on Model 2, as illustrated in Figure 5b. With an increase in the chopper frequency, the pulse energy decreases, while the pulse duration increases almost linearly. As a result, the peak power decreases rapidly, ranging from 24 kW to 70 W. A log horizontal scale is used in the peak power plot due to its large span. At a chopper frequency of 500 Hz, the output pulse energy can reach 1 mJ with a pulse duration of 42 ns, corresponding to a peak power of 24 kW. Such an intense pulse is promising for a wide range of applications.

4. Conclusions

In conclusion, we have demonstrated a mechanically Q-switched Tb:$LiYF_4$ laser based on an optical chopper. At a chopper frequency of 1 kHz and a duty cycle of 10%, the laser can generate green pulses at 544 nm with a pulse energy of 521 μJ and a pulse duration of 86 ns, corresponding to a peak power of 6.1 kW, which constitutes the highest-peak-power pulses ever achieved using Tb:$LiYF_4$ lasers to date. Further improvement in the laser performance can be expected by optimizing the coatings and choppers and increasing the pump power. When the chopper frequency and the duty cycle are increased to 10 kHz and 50%, respectively, a record average power of 874 mW is achieved. A numerical model is developed for a better understanding of the pulse dynamics, of which the accuracy has been experimentally demonstrated. The simulation results show that it is feasible to generate millijoule pulses with the peak power exceeding 10 kW. This work provides an effective way to develop high-peak-power green lasers, within which the simple, compact and economic setup should be of great interest for many applications.

Author Contributions: Conceptualization: R.Y. Funding acquisition: R.Y. Investigation: L.Y., H.Y., H.U. and R.Y. Project administration: R.Y. Resources: R.Y. Writing—original draft: L.Y., H.Y. and H.U. Writing—review and editing: R.Y. All authors have read and agreed to the published version of the manuscript.

Funding: This research was funded by the Japan Society for the Promotion of Science, grant number 23H01162.

Institutional Review Board Statement: Not applicable.

Informed Consent Statement: Not applicable.

Data Availability Statement: The data that support the findings of this study are available from the authors upon reasonable request.

Conflicts of Interest: The authors declare no conflicts of interest.

References

1. Prasad, H.S.; Brueckner, F.; Volpp, J.; Kaplan, A.F. Laser metal deposition of copper on diverse metals using green laser sources. *Int. J. Adv. Manuf. Technol.* **2020**, *107*, 1559–1568. [CrossRef]
2. Bovatsek, J.; Tamhankar, A.; Patel, R.S.; Bulgakova, N.M.; Bonse, J. Thin film removal mechanisms in ns-laser processing of photovoltaic materials. *Thin Solid Films* **2010**, *518*, 2897–2904. [CrossRef]
3. Azadgoli, B.; Baker, R.Y. Laser applications in surgery. *Ann. Transl. Med.* **2016**, *4*, 452. [CrossRef] [PubMed]
4. Mainster, M.A. Wavelength selection in macular photocoagulation: Tissue optics, thermal effects, and laser systems. *Ophthalmology* **1986**, *93*, 952–958. [CrossRef]
5. Xu, J.; Kong, M.; Lin, A.; Song, Y.; Han, J.; Xu, Z.; Wu, B.; Gao, S.; Deng, N. Directly modulated green-light diode-pumped solid-state laser for underwater wireless optical communication. *Opt. Lett.* **2017**, *42*, 1664–1667. [CrossRef]
6. Han, J.; Luo, T.; Sun, L.; Ding, C.; Xia, M.; Yang, K. Research of application of high-repetition-rate green laser in underwater imaging system. *Proc. SPIE* **2013**, *8905*, 89051Y. [CrossRef]
7. Liu, A.; Norsen, M.A.; Mead, R.D. 60-W green output by frequency doubling of a polarized Yb-doped fiber laser. *Opt. Lett.* **2005**, *30*, 67–69. [CrossRef] [PubMed]
8. Kränkel, C.; Marzahl, D.T.; Moglia, F.; Huber, G.; Metz, P.W. Out of the blue: Semiconductor laser pumped visible rare-earth doped lasers. *Laser Photonics Rev.* **2016**, *10*, 548–568. [CrossRef]
9. Tanaka, H.; Kalusniak, S.; Badtke, M.; Demesh, M.; Kuleshov, N.V.; Kannari, F.; Kränkel, C. Visible solid-state lasers based on Pr^{3+} and Tb^{3+}. *Prog. Quant. Electron.* **2022**, *84*, 100411. [CrossRef]
10. Ostroumov, V.; Seelert, W. 1 W of 261 nm cw generation in a Pr^{3+}:$LiYF_4$ laser pumped by an optically pumped semiconductor laser at 479 nm. *Proc. SPIE* **2008**, *6871*, 68711K. [CrossRef]
11. Chen, H.; Yao, W.; Uehara, H.; Yasuhara, R. Graphene Q-switched Tb:$LiYF_4$ green laser. *Opt. Lett.* **2020**, *45*, 2596–2599. [CrossRef]
12. Metz, P.W.; Marzahl, D.T.; Majid, A.; Kränkel, C.; Huber, G. Efficient continuous wave laser operation of Tb^{3+}-doped fluoride crystals in the green and yellow spectral regions. *Laser Photonics Rev.* **2016**, *10*, 335–344. [CrossRef]
13. Chen, H.; Uehara, H.; Yasuhara, R. Compact deep ultraviolet frequency-doubled Tb:$LiYF_4$ lasers at 272 nm. *Opt. Lett.* **2020**, *45*, 5558–5561. [CrossRef]
14. Tanaka, H.; Kalusniak, S.; Castellano-Hernández, E.; Kränkel, C. UV-pumping and passive Q-switching of visible Tb:$LiLuF_4$ lasers. *Proc. SPIE* **2021**, *11664*, 116640G. [CrossRef]
15. Chen, H.; Yao, W.; Uehara, H.; Yasuhara, R. Actively Q-switched Tb:$LiYF_4$ green lasers. *Appl. Phys. Express* **2021**, *14*, 062002. [CrossRef]
16. Yang, H.; Chen, H.; Li, E.; Uehara, H.; Yasuhara, R. Electro-optically Q-switched operation of a high-peak-power Tb:$LiYF_4$ green laser. *Opt. Express* **2021**, *29*, 31706–31713. [CrossRef]
17. Scheps, R.; Myers, J.F. Performance of a diode-pumped laser repetitively Q-switched with a mechanical shutter. *Appl. Opt.* **1994**, *33*, 969–978. [CrossRef]
18. Xu, F.; Pan, Q.; Zhang, Y.; Zhang, R.; Chen, Y.; Yu, D.; Chen, F. Pulse high energy Fe: ZnSe laser pumped by Q-switched Er: YAG laser. *Opt. Express* **2023**, *31*, 26807–26814. [CrossRef] [PubMed]
19. Shen, Y.; Wang, Y.; Luan, K.; Chen, H.; Tao, M.; Si, J. High peak power actively Q-switched mid-infrared fiber lasers at 3 μm. *Appl. Phys. B* **2017**, *123*, 105. [CrossRef]
20. Murphy, F.J.; Arbabzadah, E.A.; Bak, A.O.; Amrania, H.; Damzen, M.J.; Phillips, C.C. Optical chopper Q-switching for flashlamp-pumped Er,Cr:YSGG lasers. *Laser Phys. Lett.* **2015**, *12*, 045802. [CrossRef]
21. Karki, K.; Fedorov, V.; Martyshkin, D.; Mirov, S. High energy (0.8 J) mechanically Q-switched 2.94 μm Er:YAG laser. *Opt. Express* **2021**, *29*, 4287–4295. [CrossRef] [PubMed]

22. Uehara, H.; Tsunai, T.; Han, B.Y.; Goya, K.; Yasuhara, R.; Potemkin, F.; Kawanaka, J.; Tokita, S. 40 kHz, 20 ns acousto-optically Q-switched 4 μm Fe:ZnSe laser pumped by a fluoride fiber laser. *Opt. Lett.* **2020**, *45*, 2788–2791. [CrossRef] [PubMed]
23. Degnan, J.J. Theory of the optimally coupled Q-switched laser. *IEEE J. Quantum Electron.* **1989**, *25*, 214–220. [CrossRef]
24. Yamashita, T.; Ohishi, Y. Amplification and lasing characteristics of Tb^{3+}-doped fluoride fiber in the 0.54 μm band. *Jpn. J. Appl. Phys.* **2007**, *46*, L991–L993. [CrossRef]
25. Liu, J.; Wang, C.; Du, C.; Zhu, L.; Zhang, H.; Meng, X.; Wang, J.; Shao, Z.; Jiang, M. High-power actively Q-switched Nd:$GdVO_4$ laser end-pumped by a fiber-coupled diode-laser array. *Opt. Commun.* **2001**, *188*, 155–162. [CrossRef]
26. Krausz, F.; Wintner, E.; Schmidt, A.J.; Dienes, A. Continuous wave thin plate Nd:glass laser. *IEEE J. Quantum Electron.* **1990**, *26*, 158–168. [CrossRef]
27. Bezotosnyi, V.V.; Cheshev, E.A.; Gorbunkov, M.V.; Koromyslov, A.L.; Kostryukov, P.V.; Krivonos, M.S.; Popov, Y.M.; Tunkin, V.G. Behavior of threshold pump power of diode end-pumped solid-state lasers in critical cavity configurations. *Laser Phys. Lett.* **2015**, *12*, 025001. [CrossRef]